

TITLE PAGE

Chloride is an Agonist of Group II and III Metabotropic Glutamate Receptors

AUTHORS

John O. DiRaddo, Eric J. Miller, Carrie Bowman-Dalley, Barbara Wroblewska, Monica Javidnia, Ewa Grajkowska, Barry B. Wolfe, Dennis C. Liotta, Jarda T. Wroblewski

Department of Chemistry, Emory University, Atlanta, GA 30322, USA: J.O.D., E.J.M., D.C.L.

Department of Pharmacology, Georgetown University, Washington, D.C. 20057, USA: J.O.D., C.B., B.W., M.J., E.G., B.B.W., J.T.W.

RUNNING TITLE PAGE

Chloride is an Agonist of Group II and III mGlu Receptors

Correspondence should be addressed to Jarda T. Wroblewski

Department of Pharmacology

Georgetown University

Medical-Dental Building

Room #SW407

Washington, D.C. 20057, USA

Telephone: (202) 687-1566

Fax: (202) 687-8825

Email: wroblewj@georgetown.edu

Number of Text Pages: 31

Number of Tables: 0

Number of Figures: 7

Number of References: 39

Number of Words in Abstract: 146

Number of Words in Introduction: 522

Number of Words in Discussion: 1445

Nonstandard Abbreviations: AC, adenylyl cyclase; ANP, atrial natriuretic peptide; CHO, Chinese hamster ovary; CNS, central nervous system; CPPG, (*RS*)- α -Cyclopropyl-4-phosphonophenylglycine; DMEM, Dulbecco's modified eagle medium; ECD, extracellular domain; EGlu, (2*S*)-2-amino-2-ethylpentanedioic acid; FBS, fetal bovine serum; GPCR, g protein-coupled receptor; GPT, glutamate-pyruvate transaminase;

LY341495, 2-[(1S,2S)-2-carboxycyclopropyl]-3-(9H-xanthen-9-yl)-*D*-alanine; mGlu, metabotropic glutamate; PAM, positive allosteric modulator; PTX, pertussis toxin

ABSTRACT

The elemental anion chloride is generally considered a passive participant in neuronal excitability, and has never been shown to function as an agonist in its own right. We show that antagonist-mediated, glutamate-independent inverse-agonism of group II and III mGlu receptors results from inhibition of chloride-mediated activation. *In silico* molecular modeling, site-directed mutagenesis, and functional assays demonstrate (1) that chloride is an agonist of mGlu3, mGlu4, mGlu6, and mGlu8 receptors with its own orthosteric site, and (2) that chloride is not an agonist of mGlu2 receptors. Molecular modeling predicted, and site-directed mutagenesis supported that this unique property of mGlu2 receptors results from a single divergent amino acid, highlighting a molecular switch for chloride-insensitivity that is transduced through an “Arginine Flip.” Ultimately, these results suggest that activation of group II and III mGlu receptors is mediated not only by glutamate, but also by physiologically relevant concentrations of chloride.

INTRODUCTION

Cells in the central nervous system (CNS) are functionally dependent on fluctuations of elemental ions. While endogenous cations participate in propagating action potentials, they can also directly modulate receptor activity. For example, calcium flux through NMDA receptors influences neuronal depolarization (Traynelis *et al.*, 2010), modulates mGlu1 receptor activation (Jiang *et al.*, 2014), and activates the Ca^{+2} -sensing receptor (Brown *et al.*, 1993). In contrast, the elemental anion chloride is generally considered an essential, but passive participant in neuronal excitability, and, to our knowledge, it has never been shown to function as an agonist of any receptor in its own right. Chloride has, however, been shown to modulate receptor function. For example, the kainate receptors require a chloride ion between protomers to facilitate dimerization (Chaudhry *et al.*, 2009). It has also been shown that the binding of atrial natriuretic peptide (ANP) to ANP receptors requires chloride (Misono *et al.*, 2011), and that the presence of chloride influences ANP receptor oligomerization (Ogawa *et al.*, 2010). Interestingly, it has been reported that the ANP receptor chloride binding site is structurally conserved at metabotropic glutamate (mGlu) receptors (Ogawa *et al.*, 2010; Acher *et al.*, 2011).

mGlu receptors are a family of class C G protein-coupled receptors (GPCR), which is subdivided into three groups based on pharmacology, sequence homology, and signal transduction. While group I (mGlu1 and mGlu5 (IUPHAR = mGlu₁, mGlu₅)) receptors are G_q-coupled, group II (mGlu2 and mGlu3 (IUPHAR = mGlu₂, mGlu₃)) receptors and group III (mGlu4, mGlu6, mGlu7, and mGlu8 (IUPHAR = mGlu₄, mGlu₆, mGlu₇, mGlu₈)) receptors are G_{i/o}-coupled (Conn and Pin, 1997; Sharman *et al.*, 2013). While the literature is consistent regarding calcium-mediated modulation of mGlu1 receptors (Saunders *et al.*, 1998; Jiang *et al.*, 2014), the contribution of ions to group II and III mGlu receptor signaling is less clear. For example, one study concluded that mGlu3 receptors are activated by calcium (Kubo *et al.*, 1998), while another study claims that ZnCl₂, not calcium, affects radioligand binding at mGlu2, but not mGlu3, receptors (Schweitzer *et al.*, 2000). In previous work, we reported that the removal of chloride increased agonist efficacy at mGlu3 receptors (DiRaddo *et al.*, 2014). As a confounding variable, group II and III mGlu receptors have been notoriously difficult to study (Schweitzer *et al.*, 2000; Niswender *et al.*, 2008; DiRaddo *et al.*, 2014), resulting in inconsistent reports of ligand potency and affinity (Conn and Pin,

1997; Schoepp *et al.*, 1999), and several accounts of inverse agonism (Ma *et al.*, 1997; Suzuki *et al.*, 2007; DiRaddo *et al.*, 2014).

Because mGlu receptors are important regulators of neuronal signaling and promising drug targets, we examined the effects of chloride on group II and III receptors. We found that the antagonist-mediated inverse-agonism of group II and III mGlu receptors, observed in transfected CHO cells and primary cultures of rat cerebellar astrocytes, is actually due to functional competition with chloride. Using a combination of a recently reported, real-time cAMP assay (DiRaddo *et al.*, 2014), site-directed mutagenesis, and *in silico* molecular modeling, we discovered that chloride is an agonist at mGlu3, mGlu4, mGlu6 and mGlu8, receptors while mGlu2 receptors uniquely, are not activated by chloride. Furthermore, we confirm the presence of an orthosteric chloride site, and describe the structural basis of mGlu2 receptor chloride-insensitivity.

MATERIALS AND METHODS

Materials. Forskolin, *L*-glutamic acid, (2*S*)-2-Amino-2-[(1*S*,2*S*)-2-carboxycycloprop-1-yl]-3-(xanth-9-yl) propanoic acid (LY341495), (2*S*)- α -Ethylglutamic acid (EGlu), (*RS*)- α -Cyclopropyl-4-phosphonophenylglycine (CPPG), and pertussis toxin (PTX) were purchased from Tocris Bioscience (Ellisville, MO). Pyruvate, NaCl, KCl, CaCl₂, MgCl₂, NaHCO₃, HEPES, NaGluconate, KGluconate, CaGluconate₂, MgGluconate₂, NaMeSO₃, KMeSO₃, gluconic acid, proline, and TPP tissue culture plasticware were purchased from Sigma-Aldrich (St. Louis, MO). *D*-Luciferin potassium salt was purchased from Gold Biotechnology (St. Louis, MO). Dulbecco's modified Eagle's medium (DMEM), fetal bovine serum (FBS), antibiotic/antimycotic, and dialyzed FBS for tissue cultures were purchased from Invitrogen (Carlsbad, CA). Glutamate pyruvate transaminase (GPT) was purchased from Roche Diagnostics (Indianapolis, IN). All buffers were made using ultrapure H₂O from a Milli-Q water purification system (EMD Millipore, Billerica, MA).

Cell Cultures. Chinese hamster ovary (CHO) cells were transfected with the pGloSensor-22F plasmid (Promega, Madison, WI), and a stable cell line was obtained (CHO-Glo). CHO-Glo cells were then transfected with pIRES-AcGFP1 (Clontech, Mountain View, CA) encoding mGlu2, mGlu3, mGlu4, mGlu6, or mGlu8 receptors (mGlu-Glo), and cell lines were established and maintained as previously described (DiRaddo *et al.*, 2014). Rat cerebellar astrocyte cultures were prepared as previously described (Wroblewska *et al.*, 1998). In brief, dissociated cerebellar cells from 7 day old female rat pups were trypsin digested and grown in DMEM containing 10% FBS on 60 mm TPP dishes, where the medium was exchanged every 3-5 days. Cells were assayed after 9-12 days *in vitro*. The use of animals was reviewed and approved by Georgetown IACUC.

GloSensor Assay. With the exception of the GPT assay, all GloSensor assays were performed in either Locke's buffer or a modified Locke's buffer to substitute chloride. Chloride was replaced by substituting chloride salts (NaCl, KCl, CaCl₂, and MgCl₂) with gluconate salts (NaGluconate, KGluconate, CaGluconate₂, and MgGluconate₂) or, when noted, MeSO₃⁻ salts (NaMeSO₃ and KMeSO₃) or HCO₃⁻ salts

(NaHCO₃). GloSensor assays were performed as previously described (DiRaddo *et al.*, 2014). In brief, cells were plated on white-walled, clear bottom 96-well plates and grown to confluency. Culture medium was replaced with the appropriate Locke's buffer containing 1.8 mg/ml *D*-Luciferin and incubated in the dark at room temperature for 1 hour. Baseline luminescence was quantified from each well 5 times at 2 minute intervals using the EnVision Multilabel Plate Reader (PerkinElmer Life and Analytical Sciences, Waltham, MA) with a 1 second integration time. After measuring baseline luminescence, a final concentration of 1 μM forskolin with the appropriate concentration of agonist and/or antagonist was added. Luminescence was measured every 2 minutes for 18 minutes, and the levels measured at 16 minutes were used for experimental analysis. In the experiments using PTX, cells were pretreated with vehicle or 1 μg/ml of PTX 24 hours prior to the GloSensor assay. The GPT assay protocol was similar to all other GloSensor assays, with the exception that the assay was performed in DMEM containing 10% dialyzed FBS, 1.8 mg/ml *D*-Luciferin, 10 mM pyruvate, and vehicle or 33 μg/ml GPT (DMEM buffer). The medium on confluent cells was replaced with DMEM buffer with or without GPT and returned to the incubator for 3 hours. These plates were then removed from the incubator and incubated in the dark at room temperature for 1 additional hour. Drugs were added in DMEM buffer after baseline readings, and luminescence was quantified as described above.

LANCE cAMP assay. cAMP production from astrocytes was measured using the LANCE cAMP kit (PerkinElmer) according to the manufacturer's instructions. Concisely, the media on cerebellar astrocytes that were grown on 60 mm TPP plates was exchanged for Locke's buffer, and plates were equilibrated to room temperature for 1 hour. Cells were scraped from the dishes and centrifuged at 1000 x g for 1 minute and washed once with Locke's buffer. The cells were resuspended in Stimulation buffer (containing a 1:100 dilution of the Alexa-Fluor 647 antibody) and mixed with drug dilutions in a ProxiPlate-384 microplate (PerkinElmer). Cells were stimulated for 30 minutes at room temperature, Detection Mix was added, and the reaction was further incubated for 1 hour at room temperature. Fluorescence was stimulated with an excitation wavelength of 340 nm, and emission was read at 615 nm and 665 nm. Data were normalized to the readings from the control emission wavelength (615 nm).

Site-Directed Mutagenesis. Mutations to mGlu receptor cDNAs were performed by PCR-based mutagenesis using the In-Fusion HD cloning system (Clontech). Briefly, for each site mutation, two PCR products were produced with 15 bp complementary at both the 3' end of the first PCR product and at the 5' end of the second PCR product (for primers, see **Supplemental Table 1**). Each point mutation was engineered into the complementary 15 bp overhangs. PCR reactions were performed using the Phusion High-Fidelity DNA Polymerase Kit (New England Biolabs, Ipswich, MA), and products were cloned into an EcoRI cutsite using the In-Fusion cloning method. Each mutation was confirmed by sequence analysis (Genewiz, South Plainfield, NJ). Vectors expressing mutant mGlu receptors were individually transfected into CHO-Glo cells using Lipofectamine LTX (Invitrogen).

Molecular Modeling. An *in silico* mGlu3 receptor model and corresponding mGlu2 receptor homology model were generated using Maestro (Maestro, 2011) within the Schrödinger 2011 software suite. The crystal structure of the homodimeric mGlu3 receptor extracellular domain (ECD) complexed with 1S,3S-ACPD (PDB ID: 2E4W) was obtained from the Protein Data Bank (Muto *et al.*, 2007). This structure was chosen over the other agonist-bound mGlu3 receptor structures for best resolution (2.40 Å) and fewest unresolved loops. One of the monomers of the symmetrical homodimeric structure was removed along with its bound ligand and all water molecules. Using ProteinPrep (Protein Preparation Wizard. Epik version 2.2; Impact version 5.7; Prime version 3.0, Schrödinger, LLC., New York, NY., 2011) within Maestro, the remaining monomer-ligand complex was preliminarily prepared for molecular modeling. Using the Prime application (Prime, 2011) in Maestro, the resulting structure was further subjected to a series of loop refinements and energy minimizations to optimize side chain geometries and orientations, which were subsequently analyzed using web-based ProCheck (Laskowski *et al.*, 1993). Using the Prime application within Maestro, the resulting mGlu3 receptor model was used as a 3D template for generating the corresponding mGlu2 receptor homology model. A web-based version of Protein BLAST was used for multiple sequence alignment of all 8 mGlu receptors, resulting in an mGlu3 and mGlu2 receptor sequence alignment that was 66% identical and 80% homologous. This alignment was imported into Prime, where all sequence gaps were left untreated, except for a three residue gap in the mGlu3 receptor sequence. Secondary structure prediction indicated α -helical character spanning this gap, and accordingly, the

single displaced α -helical residue (S503 at mGlu3 receptors, see **Supplemental Fig. 4**) was moved to the other side of the gap. Using Prime, the resulting mGlu2 receptor structure was subjected to a series of loop refinements, energy minimizations, and side chain predictions. Model specifications were again analyzed with web-based ProCheck, and an optimized mGlu2 receptor homology model was generated. The mGlu3 receptor model and corresponding mGlu2 receptor homology model were exported from Maestro as .pdb files, which were subsequently imported into PyMOL for figure preparation (The PyMOL Molecular Graphics System).

Data Analysis and Statistics. Statistical significance was assessed using a two-tailed Student's *t*-test or a one-way ANOVA with a Bonferroni post-hoc test, as appropriate. Concentration-response curves were calculated by nonlinear regression using the four-parameter logistic equation. Calculations were performed using GraphPad Prism software (La Jolla, CA).

RESULTS

Inverse agonism at group II and III mGlu receptors is not due to competition with glutamate

While establishing the GloSensor cAMP assay to measure activation of the $G_{i/o}$ -coupled mGlu receptors (DiRaddo *et al.*, 2014), we observed that, relative to vehicle treatment, the nonselective, competitive antagonist LY341495, significantly increased forskolin-stimulated cAMP production in mGlu3-, mGlu4-, mGlu6-, and mGlu8-, but not mGlu2-, Glo cell lines (**Fig. 1A-E, bars**). Although we have successfully expressed mGlu7 receptors, a functional mGlu7-Glo cell line remains elusive (DiRaddo *et al.*, 2014). Pretreatment with pertussis toxin (PTX) completely eliminated the effect of LY341495 (**Fig. 1A-E, bars**), indicating that this antagonist-mediated increase in cAMP was due to $G_{\alpha_{i/o}}$ signaling, and resulted from a disinhibition of adenylyl cyclase (AC). Concentration-response curves of LY341495, EGlu (a group II-selective antagonist), and CPPG (a group III-selective antagonist) demonstrated dose-dependency, confirming that inverse agonism is mGlu receptor-mediated and not unique to LY341495 (**Fig. 1A-E, curves**). These results encouraged us to determine whether LY341495 could disinhibit cAMP production in a native system. Indeed, in primary cultures of cerebellar astrocytes, LY341495 increased forskolin-stimulated cAMP levels, and furthermore, glutamate did not significantly inhibit cAMP production (**Fig. 1F**). This result is consistent with our work in transfected cells (DiRaddo *et al.*, 2014), and could indicate that antagonists of mGlu3, mGlu4, mGlu6, and mGlu8 receptors are actually inverse-agonists of high constitutive GPCR activity (~80% at mGlu3 and mGlu8 receptors).

Alternatively, antagonists could have been competing with residual glutamate. Therefore, experiments were performed using glutamate-pyruvate transaminase (GPT), an enzyme that converts glutamate to an inactive metabolite, α -ketoglutarate. Concentration-response curves of LY341495 at mGlu3 receptors showed statistically indistinguishable potencies in the absence ($EC_{50} = 21$ nM) and presence ($EC_{50} = 14$ nM) of GPT (**Fig. 2A**). In the presence of 30 μ M glutamate, however, the concentration-response curve of LY341495 was shifted 9-fold to the right ($EC_{50} = 420$ nM) without GPT, relative to the control ($EC_{50} = 47$ nM) with GPT (**Fig. 2B**). If antagonist-mediated efficacy were due to competition with residual glutamate, LY341495 potency would be statistically different in the presence of GPT, or LY341495 efficacy would be absent. In contrast, our results show no change in potency.

Additionally, our data show an increase in LY341495 efficacy with GPT treatment, possibly due to supersensitization of AC (Watts and Neve, 2005; DiRaddo *et al.*, 2014). These results indicate that the antagonist-mediated efficacy observed in **Figure 1** was not due to competition with glutamate; rather, it represents either true inverse-agonism of constitutive mGlu receptor activity, or competition with an unidentified agonist.

Chloride activates mGlu3, mGlu4, mGlu6, and mGlu8 receptors at its own orthosteric site, which is disrupted at mGlu2 receptors.

We previously showed that chloride replacement (with gluconate) improved agonist efficacy at mGlu3 receptors (DiRaddo *et al.*, 2014). To determine that this effect was, in fact, due to chloride removal and not gluconate addition, experiments were performed using structurally distinct anion substitutions. Substitution of chloride with gluconate or methanesulfonate at all receptors, as well as bicarbonate at mGlu3 receptors, revealed statistically indistinguishable results (**Supplemental Fig. 1A-E**), confirming that this effect was chloride-specific. To investigate the effects of chloride on the activation of group II and III mGlu receptors, buffers containing increasing concentrations of chloride (replaced with gluconate) were employed. To compare chloride concentration-response curves between different cell lines, results were normalized to maximal cAMP production at each chloride concentration (i.e. **Fig. 3A** vs. **Supplemental Fig. 2A**). As halides are known to affect AC activity (Kalish *et al.*, 1974), this method of normalization accounts for receptor-independent effects of chloride on AC (see raw data in **Supplemental Fig. 2**) and results in concentration-response curves that represent only chloride-mediated activation of the indicated mGlu receptors. As a negative control, a saturating concentration (10 μ M) of the orthosteric mGlu receptor antagonist, LY341495 was employed to measure receptor-independent cAMP production. Additionally, a saturating concentration of glutamate (1 mM) was used as a positive control to establish the maximal level of mGlu receptor-mediated inhibition of cAMP production. Using this experimental paradigm, increasing chloride concentrations revealed a concentration-dependent chloride-mediated activation of mGlu3 ($EC_{50} = 29$ mM), mGlu4 ($EC_{50} = \sim 280$ mM), mGlu6 ($EC_{50} = \sim 120$ mM), and mGlu8 ($EC_{50} = 21$ mM), but not mGlu2, receptors (**Fig. 3B-F**). Standard errors and hill slopes are reported in **Supplemental Table 2**. cAMP levels in CHO-Glo cells were unaffected by 10 μ M LY341495

or 1 mM glutamate, regardless of chloride concentration (**Fig. 3A**). Maximal cAMP inhibition by glutamate was variable between receptor subtypes, possibly due to different transfection or G_{V_o} -coupling efficiencies between cell-lines or receptor subtypes, respectively. At mGlu3 and mGlu8 receptors, these data indicate that chloride and glutamate inhibit cAMP production to the same degree and that high chloride concentrations produce maximal receptor activation which is neither additive with nor affected by glutamate. We conclude that chloride independently activates mGlu3, mGlu4, mGlu6, and mGlu8, but not mGlu2, receptors.

We then hypothesized that the previously reported “putative chloride binding site (Acher *et al.*, 2011)” is, in fact, the orthosteric pocket for chloride. Although no crystal structures of the extracellular domains (ECD) of mGlu2, mGlu4, mGlu6, or mGlu8 receptors are available, several agonist-bound mGlu3 receptor ECD crystal structures have been published (Muto *et al.*, 2007). Unfortunately, the corresponding x-ray structures do not show chloride occupation of the putative site; rather, this pocket is occupied by a water molecule. In contrast, an unpublished crystal structure of the mGlu3 receptor ECD bound to LY341495 (PDB ID: 3SM9) does contain a chloride ion in the “putative chloride binding site.” Comparison between the agonist-bound and antagonist-bound structures revealed that the residues comprising this site were identically aligned, and furthermore, that the respective water molecule and chloride ion were oriented precisely. To illustrate the proximity of the “putative chloride binding site” and orthosteric glutamate (**Data Supplement 1**), **Figure 4A** displays the glutamate-bound crystal structure of the mGlu3 receptor ECD (PDB ID: 2E4U) where the water molecule (**Data Supplement 2**) is colored green to represent chloride.

Although it has been proposed that the “putative chloride binding site” may exist at all group II and III mGlu receptors (Ogawa *et al.*, 2010; Acher *et al.*, 2011), our data show that mGlu2 receptors are not activated by chloride. Thus, we hypothesized that the “putative chloride binding site” present at mGlu3 receptors is disrupted at mGlu2 receptors. To initially evaluate this hypothesis, we generated an *in silico* model of the mGlu3 receptor ECD (**Data Supplement 3**), using Maestro (Maestro, 2011) in the Schrödinger software suite, and built a corresponding homology model of the mGlu2 receptor (**Data Supplement 4**) using the Prime application (Prime, 2011) in Maestro. Our mGlu3 receptor model overlaid with the water molecule (colored green to represent chloride) from PDB ID:2E4U shows that chloride is

appropriately positioned for hydrogen bonding interactions with the polar hydrogen of the T98 side chain, as well as with the polar hydrogens of the Y150 and S149 backbone nitrogens (**Fig. 4B**). Alternatively, our mGlu2 receptor homology model shows significant differences in the conformations of the corresponding residues (S91, Y144, and S143), all of which are improperly aligned for hydrogen bonding interactions with chloride (**Fig. 4C**). An overlay of these models (**Fig. 4D**) suggests that a backbone shift (indicated with arrows) is responsible for these conformational differences, and ultimately for mGlu2 receptor chloride-insensitivity.

While the “putative chloride binding site” is strongly implicated as the orthosteric chloride pocket, chloride interaction at this site has never been validated empirically. In principle, mutation of T98 to a larger and negatively charged aspartate residue should sterically and electrostatically preclude chloride function. Accordingly, we constructed an mGlu3 receptor T98D mutant, which, unlike wild-type mGlu3 receptors, showed considerably less LY341495-mediated inverse agonism ($p=0.048$) in the presence of 125 mM chloride, as well as a strong response to glutamate treatment (**Fig. 4E**). Also in contrast to the wild-type receptor, the mutant receptor responded to both drugs in a chloride-independent manner. This not only demonstrates that T98 is critical for chloride binding, but ultimately supports the hypothesis that the “putative chloride binding site” is, in fact, the orthosteric binding pocket for chloride. Because T98 is conserved as either a threonine or serine at all group II and III mGlu receptors (**Supplemental Fig. 4**), it is probable that chloride-mediated activation of mGlu4, mGlu6, and mGlu8 receptors also results from chloride binding in this orthosteric region.

Chloride is an agonist of mGlu3 and mGlu8 receptors, and an agonist and positive allosteric modulator (ago-PAM) of mGlu4 and mGlu6 receptors.

To investigate the relationship between the two agonists, glutamate and chloride, concentration-response curves of glutamate at several chloride concentrations were generated (**Fig. 5A-D**). The parameters E_{max} , E_0 , and EC_{50} were analyzed for statistically significant differences (**Fig. 5E**). The results show no significant difference in E_{max} of glutamate at mGlu3, mGlu4, mGlu6, or mGlu8 receptors, suggesting that glutamate efficacy is unaffected by chloride. However, E_0 increased in response to increasing concentrations of chloride. These data further support that chloride activates mGlu3, mGlu4,

mGlu6, and mGlu8 receptors in the absence of glutamate, and that both ligands are agonists of these receptors. Finally, EC_{50} values for glutamate at mGlu4 and mGlu6 receptors were statistically different with increasing chloride, suggesting that chloride acts as a positive allosteric modulator (PAM) of glutamate activity at these receptors. In contrast, glutamate EC_{50} values at mGlu3 and mGlu8 receptors appeared to be statistically unaffected (**Fig. 5E**).

An “Arginine Flip,” elicited by a single residue difference, dictates the selectivity of chloride for mGlu3 versus mGlu2 receptors

Next, we sought to understand the structural basis for chloride-insensitivity at mGlu2 receptors. Preliminary comparison of our mGlu3 receptor model and corresponding mGlu2 receptor homology model illustrated a change in backbone conformation that appears to preclude chloride binding at mGlu2 receptors (**Fig. 4D**). Further analysis revealed that this backbone shift stems from a stark conformational difference between corresponding arginine and tyrosine residues, R277/Y150 and R271/Y144, at the mGlu3 and mGlu2 receptor models, respectively (**Fig. 6A**). The mGlu3 receptor model shows that R277 interacts with Y150, one of the key residues in the orthosteric chloride pocket, via a π -cation interaction (**Fig. 6B**). At the mGlu2 receptor model however, R271 adopts a conformation that precludes a π -cation interaction (**Fig. 6B**), causing Y144 to adopt a different orientation that leads to the aforementioned backbone shift. Consequently, this “Arginine Flip,” which appears to be mediated by two homologous amino acids that are different between mGlu2 and mGlu3 receptors, disrupts the orthosteric chloride site at mGlu2 receptors. While the conformation of R277 at mGlu3 receptors is stabilized by a salt bridge with D279 (E273 at mGlu2 receptors), the orientation of R271 at mGlu2 receptors is stabilized by a salt bridge with D146 (S152 at mGlu3 receptors). As D146 is a unique residue of mGlu2 receptors (a conserved serine at all other mGlu receptors, **Supplemental Fig. 4**), we hypothesized that D146 and S152 are responsible for chloride discrimination between mGlu2 and mGlu3 receptors. To test this hypothesis empirically, an mGlu2 receptor D146S mutant and the corresponding mGlu3 receptor S152D mutant were constructed. In support of our hypothesis, and in contrast to the wild-type mGlu2 receptor (**Fig. 7A**), the D146S mutant, was activated by chloride (**Fig. 7C**). The converse mutation at mGlu3 receptors (S152D) however, resulted in a chloride-insensitive, constitutively active receptor (**Fig. 7D**). Based on this

unexpected constitutive activity, we broadened our hypothesis to include E273 and D279 as residues responsible for chloride discrimination between mGlu2 and mGlu3 receptors, respectively. Accordingly, a new series of mGlu2 receptor mutants (E273D and D146S/E273D) and corresponding mGlu3 receptor mutants (D279E and S152D/D279E) were constructed. The mGlu2 receptor E273D mutant was chloride-insensitive (**Supplemental Fig. 2A**), and similar to the wild-type mGlu2 receptor. The mGlu3 receptor D279E mutant however, showed a rightward shift in chloride potency (**Supplemental Fig. 2B**), suggesting that the larger glutamate residue partially destabilizes the π -cation interaction between Y150 and R277, relative to wild-type mGlu3 receptors. The mGlu2 receptor D146S/E273D mutant (**Supplemental Fig. 2C**) showed similar chloride-sensitivity to that observed at the mGlu2 receptor D146S mutant, suggesting that E273 does not participate in stabilizing the conformation of R271. Conversely, the mGlu3 receptor S152D/D279E mutant was neither chloride-sensitive nor constitutively active (**Fig. 7E**), effectively resulting in an mGlu3 receptor that behaved like a wild-type mGlu2 receptor. These results demonstrate that the single structural determinant of chloride-insensitivity at mGlu2 receptors is D146, which facilitates the R271 “Arginine Flip,” thereby precluding a π -cation interaction with Y144. These findings strongly suggest that the π -cation interaction between R277 and Y150 structurally rigidifies the orthosteric chloride site at mGlu3 receptors, and that the absence of a similar interaction at mGlu2 receptors prevents chloride-mediated activation.

DISCUSSION

Our group and others have reported antagonist-mediated increases in cAMP production at group II and III mGlu receptors (Ma *et al.*, 1997; Suzuki *et al.*, 2007; DiRaddo *et al.*, 2014). In agreement with Suzuki *et al.*, our data show that antagonist-mediated efficacy is PTX-sensitive (Suzuki *et al.*, 2007), indicating an already engaged $G_{\alpha_{i/o}}$ -coupled signaling mechanism. Furthermore, we observed LY341495-mediated inverse agonism in primary cultures of cerebellar astrocytes, suggesting that, even in the absence of glutamate, these receptors are highly active *in vivo*. Our data demonstrate that high basal group II and III mGlu receptor activity is not due to glutamate contamination, but is rather due to the presence of the endogenous agonist, chloride. Before the mGlu receptors were cloned, several studies reported that chloride enhanced [3 H]-glutamate binding in rat brain (Mena *et al.*, 1982), and also in astrocytes at binding sites that were unaffected by kainate and NMDA (Bridges *et al.*, 1987). Since, it has been reported that radioligand binding to truncated mGlu3 and mGlu4 receptors was improved by physiologically relevant chloride concentrations (Kuang and Hampson, 2006). In contrast, other studies have suggested that cations affect group II mGlu receptors (Kubo *et al.*, 1998; Schweitzer *et al.*, 2000). Kubo *et al.* concluded that increasing concentrations of Ca^{+2} (counterion not specified) activated mGlu3, but not mGlu2, receptors (Kubo *et al.*, 1998), although the concurrent increase in chloride concentration was not controlled for. To our knowledge, no functional studies have controlled for chloride concentration while measuring activation of these receptors. Because nearly all physiological buffers contain chloride, it is likely that chloride has been a confounding variable in many reports of group II and III mGlu receptor activation. While our previous data show that calcium does not modulate glutamate-mediated group II or III mGlu receptor activity (DiRaddo *et al.*, 2014), our current results demonstrate that chloride activates mGlu3, mGlu4, mGlu6, and mGlu8, but not mGlu2, receptors. Because receptor activation results from direct interaction of the endogenous ion chloride with its own binding site, chloride is, by definition, an orthosteric agonist of these mGlu receptors. Chloride also potentiates glutamate potency at mGlu4 and mGlu6 receptors, and therefore, chloride is a PAM with respect to glutamate activity at these receptors. Future experiments will clarify not only whether glutamate is a PAM with respect to chloride, but also how chloride modulates the potency of other orthosteric ligands. Ultimately, our data show that, with the

exception of mGlu2 receptors, the group II and III mGlu receptors are as much chloride receptors as they are glutamate receptors.

Interestingly, the chloride binding site at group II and III mGlu receptors is structurally conserved at ANP receptors (Acher *et al.*, 2011; Misono *et al.*, 2011). While chloride is not an agonist of ANP receptors, chloride has been shown to modulate ANP receptor oligomerization (Ogawa *et al.*, 2010). In the absence of chloride, ANP receptors are exclusively dimerized, regardless of receptor number. In the presence of 150 mM chloride however, free monomers predominate, but shift towards the dimeric state as a function of increasing receptor expression. Preliminary competition binding experiments revealed complex chloride-dependent effects on both ligand potency and the number of glutamate binding sites at mGlu3 receptors (data not shown). Further investigation will determine if a similar phenomenon underscores a dynamic interplay between monomeric, homodimeric, and heterodimeric mGlu receptor states, regulated by both chloride concentration and receptor expression.

Because mGlu2 receptors are the only group II and III mGlu receptors that are not activated by chloride, we propose that chloride-sensitivity is a fundamental property of these receptors, and that mGlu2 receptor chloride-insensitivity is exceptional. Our results suggest that this chloride-insensitivity stems from the absence of a π -cation interaction between R271 and Y144, which is present between R277 and Y150 at mGlu3 receptors. While this π -cation interaction has been previously described as a structural motif of both mGlu2 and mGlu3 receptors (Muto *et al.*, 2007; Lundström *et al.*, 2009), it is not absolutely required for glutamate-mediated activation (Malherbe *et al.*, 2001; Yao *et al.*, 2003; Lundström *et al.*, 2009), and our data support that it is only present at mGlu3 receptors. Instead, we propose that D146 at mGlu2 receptors (a conserved serine at all other mGlu receptors) precludes a π -cation interaction by facilitating an “Arginine Flip,” relative to mGlu3 receptors, which consequently disrupts the orthosteric chloride site. Supporting this claim is the chloride-sensitive mGlu2 receptor D146S and D146S/E273D mutants and the chloride-insensitive mGlu3 receptor S152D and S152D/D279E mutants. This swap of chloride-sensitivity by site-directed mutagenesis is consistent with other studies, where the differential ion-sensitivities of the wild-type receptors were reversed by D146S mutation at mGlu2 receptors and corresponding S152D mutation at mGlu3 receptors (Kubo *et al.*, 1998; Malherbe *et al.*, 2001). We assert that the “Arginine Flip” is induced by mutation of a single amino acid, which acts as a

chloride switch between mGlu2 and mGlu3 receptors. Because the arginine and tyrosine residues are not conserved through the group III mGlu receptors (**Supplemental Fig. 4**), this chloride switch marks a unique structural divergence between mGlu3 and mGlu2 receptors, which share 80% sequence homology, and are largely thought to activate and signal in the same fashion.

Despite a shared $G_{i/o}$ -coupled signaling mechanism, recent studies demonstrate that activation of mGlu2 and mGlu3 receptors can elicit opposing neurotrophic and cognitive effects (Taylor *et al.*, 2002, 2005; Corti *et al.*, 2007; Fell *et al.*, 2008; Caraci *et al.*, 2012). This highlights the need for subtype selective agonists to evaluate the therapeutic potential of each mGlu receptor. Unfortunately, selective activation of mGlu3 or mGlu2 receptors has been difficult to achieve due to the lack of identified structural differences. Our results demonstrate a subtle difference in tyrosine conformation that may be exploitable for drug selectivity. In support of this claim, a previous study showed that a 4-fold difference in [3 H]-LY354740 affinity between mGlu2 and mGlu3 receptors was reversed at the D146S and S152D receptor mutants, respectively (Malherbe *et al.*, 2001). Because S152 and D146 do not directly interact with agonists (Muto *et al.*, 2007), our results suggest that this affinity reversal was due to an “Arginine Flip” that alters the conformation of more proximal tyrosine. Furthermore, a new, selective mGlu2 receptor agonist has been proposed to bind near S278/S272 (Monn *et al.*, 2013), which are directly adjacent to R277/R271 at mGlu3 and mGlu2 receptors, respectively. As our models do not predict different conformations of S278 and S272, the selective mGlu2 receptor agonist may actually exploit different conformations of the neighboring tyrosine and/or arginine residues.

Our results also reveal a second region of dissimilarity between mGlu3 and mGlu2 receptors: the orthosteric chloride site. While targeting this region has already been proposed as a strategy for the design of subtype-selective group III mGlu receptor agonists (Acher *et al.*, 2011; Goudet *et al.*, 2012), mGlu4, mGlu6, and mGlu8 receptors all contain functional chloride sites. In contrast to the claim that all mGlu receptors share the “putative chloride binding site,” (Acher *et al.*, 2011) our results demonstrate that this site is not conserved at mGlu2 receptors. Thus, the opportunity for subtype-selectivity between group II mGlu receptors by targeting the orthosteric chloride site (or lack thereof) is much more pronounced than for group III mGlu receptors, where this strategy may have already had some success (Goudet *et al.*, 2012). The close proximity of the chloride pocket and glutamate binding site, as well as the effects of

chloride on glutamate potency at mGlu4 and mGlu6 receptors, renders selective orthosteric drug design inextricably intertwined with chloride function.

Chloride, an endogenous anion generally deemed a passive participant in neuronal excitability, is an agonist of mGlu3 and mGlu8 receptors and an ago-PAM of mGlu4 and mGlu6 receptors that acts at its own orthosteric pocket. Therefore, we conclude that these mGlu receptors have two, distinct orthosteric sites (Christopoulos *et al.*, 2014), one for glutamate and one for chloride. Our data show that, with the exception of mGlu2 receptors, the group II and III mGlu receptors are as much chloride receptors as they are glutamate receptors. Furthermore, chloride-insensitivity of mGlu2 receptors results from a single amino acid difference, highlighting a molecular switch for chloride-insensitivity that may be transduced through an "Arginine Flip." These structural differences between mGlu2 and mGlu3 receptors mark a new strategy for the design of subtype-selective group II mGlu receptor agonists, which must be considered within the context of chloride function. Ultimately, our findings underscore a scenario in which either (1) mGlu3, mGlu4, mGlu6, and mGlu8 receptors are highly active *in vivo* due to static extracellular chloride concentrations, or (2) as can be deduced from recent literature (Glykys *et al.*, 2014), chloride microdomains exist throughout the CNS, rendering local, extracellular, chloride levels far more tightly regulated, both spatially and temporally, than currently accepted.

ACKNOWLEDGEMENTS

We thank Dr.'s James Snyder, Haipeng Hu, and Pieter Burger for their assistance with molecular modeling.

AUTHORSHIP CONTRIBUTIONS

Participated in research design: DiRaddo, Miller, Wroblewska, Wolfe, Liotta, Wroblewski

Conducted experiments: DiRaddo, Miller, Bowman-Dalley, Wroblewska, Javidnia, Grajkowska, Wolfe

Contributed new reagents or analytical tools: DiRaddo, Miller, Wroblewska, Wolfe

Performed data analysis: DiRaddo, Miller, Bowman-Dalley, Wolfe, Wroblewski

Wrote or contributed to the writing of the manuscript: DiRaddo, Miller, Bowman-Dalley, Wroblewska, Javidnia, Wolfe, Liotta, Wroblewski

REFERENCES

- Acher FC, Selvam C, Pin J-P, Goudet C, and Bertrand H-O (2011) A critical pocket close to the glutamate binding site of mGlu receptors opens new possibilities for agonist design. *Neuropharmacology* **60**:102–107, Elsevier Ltd.
- Bridges RJ, Kesslak JP, Nieto-Sampedro M, Broderick JT, Yu J, and Cotman CW (1987) A L-[³H]glutamate binding site on glia: an autoradiographic study on implanted astrocytes. *Brain Res* **415**:163–168.
- Brown EM, Gamba G, Riccardi D, Lombardi M, Butters R, Klfor O, Sun A, Hediger MA, Lytton J, and Hebert SC (1993) Cloning and characterization of an extracellular Ca²⁺-sensing receptor from bovine parathyroid. *Nature* **366**:575–580.
- Caraci F, Battaglia G, Sortino MA, Spampinato S, Molinaro G, Copani A, Nicoletti F, and Bruno V (2012) Metabotropic glutamate receptors in neurodegeneration/neuroprotection: still a hot topic? *Neurochem Int* **61**:559–565, Elsevier Ltd.
- Chaudhry C, Plested AJR, Schuck P, and Mayer ML (2009) Energetics of glutamate receptor ligand binding domain dimer assembly are modulated by allosteric ions. *Proc Natl Acad Sci U S A* **106**:12329–12334.
- Christopoulos A, Changeux J, Catterall WA, Fabbro D, Burris TP, Cidlowski JA, and Olsen RW (2014) International Union of Basic and Clinical Pharmacology . XC . Multisite Pharmacology: Recommendations for the Nomenclature of Receptor Allosterism and Allosteric Ligands. *Pharmacol Rev* **66**:918–947.
- Conn PJ, and Pin JP (1997) Pharmacology and functions of metabotropic glutamate receptors. *Annu Rev Pharmacol Toxicol* **37**:205–237.
- Corti C, Battaglia G, Molinaro G, Rizzo B, Pittaluga A, Corsi M, Mugnaini M, Nicoletti F, and Bruno V (2007) The use of knock-out mice unravels distinct roles for mGlu2 and mGlu3 metabotropic glutamate receptors in mechanisms of neurodegeneration/neuroprotection. *J Neurosci* **27**:8297–8308.
- DiRaddo JO, Miller EJ, Hathaway H a, Grajkowska E, Wroblewska B, Wolfe BB, Liotta DC, and Wroblewski JT (2014) A real-time method for measuring cAMP production modulated by Gai/o-coupled metabotropic glutamate receptors. *J Pharmacol Exp Ther* **349**:373–382.
- Fell MJ, Svensson KA, Johnson BG, and Schoepp DD (2008) Evidence for the Role of Metabotropic Glutamate (mGlu)₂ Not mGlu₃ Receptors in the Preclinical Antipsychotic Pharmacology of the mGlu_{2/3} Receptor Agonist (–)-(1R,4S,5S,6S)-4-Amino-2-sulfonylbicyclo[3.1.0]hexane-4,6-dicarboxylic Acid (LY404039). *J Pharmacol Exp Ther* **326**:209–217.
- Glykys J, Dzhala V, Egawa K, Balena T, Saponjian Y, Kuchibhotla K V, Bacsikai BJ, Kahle KT, Zeuthen T, and Staley KJ (2014) Local impermeant anions establish the neuronal chloride concentration. *Science* **343**:670–675.
- Goudet C, Vilar B, Courtiol T, Deltheil T, Bessiron T, Brabet I, Oueslati N, Rigault D, Bertrand H-O, McLean H, Daniel H, Amalric M, Acher F, and Pin J-P (2012) A novel selective metabotropic glutamate receptor 4 agonist reveals new possibilities for developing subtype selective ligands with therapeutic potential. *FASEB J* **26**:1682–1693.

- Jiang JY, Nagaraju M, Meyer RC, Zhang L, Hamelberg D, Hall R a, Brown EM, Conn PJ, and Yang JJ (2014) Extracellular calcium modulates actions of orthosteric and allosteric ligands on metabotropic glutamate receptor 1 α . *J Biol Chem* **289**:1649–1661.
- Kalish MI, Pineryro MA, Cooper B, and Gregerman RI (1974) Adenylyl cyclase activation by halide anions other than fluoride. *Biochem Biophys Res Commun* **6**:781–787.
- Kuang D, and Hampson DR (2006) Ion dependence of ligand binding to metabotropic glutamate receptors. *Biochem Biophys Res Commun* **345**:1–6.
- Kubo Y, Miyashita T, and Murata Y (1998) Structural basis for a Ca²⁺-sensing function of the metabotropic glutamate receptors. *Science* **279**:1722–1725.
- Laskowski RA, MacArthur MW, Moss DS, and Thornton JM (1993) PROCHECK: A Program to Check the stereochemical quality of protein structures. *J Appl Crystallogr* **26**:283–291.
- Lundström L, Kuhn B, Beck J, Borroni E, Wettstein JG, Woltering TJ, and Gatti S (2009) Mutagenesis and molecular modeling of the orthosteric binding site of the mGlu2 receptor determining interactions of the group II receptor antagonist (3)H-HYDIA. *ChemMedChem* **4**:1086–1094.
- Ma D, Tian H, Sun H, Kozikowshi AP, Pshenichkin S, and Wroblewski JT (1997) Synthesis and Biological Activity of Cyclic Analogues of MPPG and MCPG as Metabotropic Glutamate Receptor Antagonists. *Bioorganic Med Chem Lett* **7**:1195–1198.
- Maestro (2011) . Version 9.2, Schrödinger, LLC., New York, NY.
- Malherbe P, Knoflach F, Broger C, Ohresser S, Kratzeisen C, Adam G, Stadler H, Kemp J a, and Mutel V (2001) Identification of essential residues involved in the glutamate binding pocket of the group II metabotropic glutamate receptor. *Mol Pharmacol* **60**:944–954.
- Mena EE, Fagg GE, and Cotman CW (1982) Chloride ions enhance L-glutamate binding to rat brain synaptic membranes. *Brain Res* **243**:378–381.
- Misono KS, Philo JS, Arakawa T, Ogata CM, Qiu Y, Ogawa H, and Young HS (2011) Structure, signaling mechanism and regulation of the natriuretic peptide receptor guanylate cyclase. *FEBS J* **278**:1818–1829.
- Monn JA, Valli MJ, Massey SM, Hao J, Reinhard MR, Bures MG, Heinz BA, Wang X, Carter JH, Getman BG, Stephenson GA, Herin M, Catlow JT, Swanson S, Johnson BG, Mckinzie DL, and Henry SS (2013) Synthesis and Pharmacological Characterization of 4-Substituted-2-Aminobicyclo[3.1.0]hexane-2,6-dicarboxylates: Identification of New Potent and Selective Metabotropic Glutamate 2/3 Receptor Agonists. *J Med Chem* **56**:4442–4455.
- Muto T, Tsuchiya D, Morikawa K, and Jingami H (2007) Structures of the extracellular regions of the group II/III metabotropic glutamate receptors. *Proc Natl Acad Sci U S A* **104**:3759–3764.
- Niswender CM, Johnson KA, Luo Q, Ayala JE, Kim C, Conn PJ, and Weaver CD (2008) A Novel Assay of Gi/o-Linked G Protein-Coupled Receptor Coupling to Potassium Channels Provides New Insights into the Pharmacology of the Group III Metabotropic Glutamate Receptors. *Mol Pharmacol* **73**:1213–1224.

- Ogawa H, Qiu Y, Philo JS, Arakawa T, Ogata CM, and Misono KS (2010) Reversibly bound chloride in the atrial natriuretic peptide receptor hormone-binding domain: possible allosteric regulation and a conserved structural motif for the chloride-binding site. *Protein Sci* **19**:544–557.
- Prime (2011) . Version 3.0, Schrödinger, LLC., New York, NY.
- Protein Preparation Wizard. Epik version 2.2; Impact version 5.7; Prime version 3.0, Schrödinger, LLC., New York, NY. (2011).
- Saunders R, Nahorski SR, and Challiss RAJ (1998) A modulatory effect of extracellular Ca²⁺ on type 1α metabotropic glutamate receptor-mediated signalling. *Neuropharmacology* **37**:273–276.
- Schoepp DD, Jane DE, and Monn J a (1999) Pharmacological agents acting at subtypes of metabotropic glutamate receptors. *Neuropharmacology* **38**:1431–1476.
- Schweitzer C, Kratzeisen C, Adam G, Lundstrom K, Malherbe P, Ohresser S, Stadler H, Wichmann J, Woltering T, and Mutel V (2000) Characterization of [(3)H]-LY354740 binding to rat mGlu2 and mGlu3 receptors expressed in CHO cells using semliki forest virus vectors. *Neuropharmacology* **39**:1700–1706.
- Sharman JL, Spedding M, Peters J a, and Harmar AJ (2013) The Concise Guide To Pharmacology 2013/14: G Protein-Coupled Receptors. *Br J Pharmacol* **170**:1459–1581.
- Suzuki G, Tsukamoto N, Fushiki H, Kawagishi A, Nakamura M, Kurihara H, Mitsuya M, Ohkubo M, and Ohta H (2007) In Vitro Pharmacological Characterization of Novel Isoxazolopyridone Derivatives as Allosteric Metabotropic Glutamate Receptor 7 Antagonists. *J Pharmacol Exp Ther* **323**:147–156.
- Taylor D, Diemel L, and Cuzner M (2002) Activation of group II metabotropic glutamate receptors underlies microglial reactivity and neurotoxicity following stimulation with chromogranin A, a peptide upregulated in Alzheimer's disease. *J Neurochem* **82**:1179–1191.
- Taylor DL, Jones F, Kubota ESFCS, and Pocock JM (2005) Stimulation of microglial metabotropic glutamate receptor mGlu2 triggers tumor necrosis factor alpha-induced neurotoxicity in concert with microglial-derived Fas ligand. *J Neurosci* **25**:2952–2964.
- The PyMOL Molecular Graphics System (n.d.) . Version 1.5.0.4, Schrödinger, LLC., New York, NY.
- Traynelis SF, Wollmuth LP, McBain CJ, Menniti FS, Vance KM, Ogden KK, Hansen KB, Yuan H, Myers SJ, and Dingledine R (2010) Glutamate Receptor Ion Channels: Structure , Regulation , and Function. *Pharmacol Rev* **62**:405–496.
- Watts VJ, and Neve KA (2005) Sensitization of adenylate cyclase by Galpha i/o-coupled receptors. *Pharmacol Ther* **106**:405–421.
- Wroblewska B, Santi MR, and Neale JH (1998) N-Acetylaspartylglutamate Activates Cyclic AMP-Coupled Metabotropic Glutamate Receptors in Cerebellar Astrocytes. *Glia* **24**:172–179.
- Yao Y, Pattabiraman N, Michne WF, Huang X-P, and Hampson DR (2003) Molecular modeling and mutagenesis of the ligand-binding pocket of the mGlu3 subtype of metabotropic glutamate receptor. *J Neurochem* **86**:947–957.

FOOTNOTES

Some information presented herein is in John O. DiRaddo's Ph.D. Thesis (unpublished until July 2015) and Eric J. Miller's Ph.D. Thesis (scheduled for August 2015). Also, some information was presented during a poster session by John O. DiRaddo and Eric J. Miller at the "8th International Meeting on Metabotropic Glutamate Receptors," on September 30, 2014.

FIGURE LEGENDS

Figure 1. LY341495 (495) disinhibits forskolin-stimulated cAMP production via group II and III mGlu receptors. **(A-E, bars)** The nonselective, competitive antagonist LY341495 (10 μ M), significantly increased forskolin-stimulated cAMP levels in mGlu3-, mGlu4-, mGlu6-, and mGlu8-, but not mGlu2-, Glo cell lines. When these cell lines were pretreated with pertussis toxin (PTX) however, this apparent inverse-agonism was absent. Maximal cAMP production was independently normalized in the absence of or presence of PTX. **(A-E, curves)** Concentration-response curves of LY341495 demonstrate dose-dependence, and concentration-response curves of either EGlu or CPPG demonstrate specificity for group II and III mGlu receptors, respectively. cAMP levels, stimulated with 1 μ M forskolin, were measured by the GloSensor method. **(F)** In primary cultures of rat cerebellar astrocytes, treatment with 10 μ M LY341495 significantly increased cAMP levels, indicating a similar disinhibition of adenylyl cyclase as observed in mGlu-Glo cells. cAMP levels, stimulated with 1 μ M forskolin were measured by the LANCE method and calculated relative to a cAMP standard curve. Data are normalized to maximal cAMP levels and are presented as the mean \pm S.E.M. of three individual experiments performed in triplicate. Statistical significance was assessed using a two-tailed Student's *t*-test. *** $P < 0.001$.

Figure 2. LY341495-mediated increases in cAMP levels are not due to competition with glutamate. **(A)** Concentration-response curves of LY341495 in the absence or presence of GPT show no statistical difference in antagonist potency. **(B)** When spiked with 30 μ M glutamate, concentration-response curves of LY341495 in the absence of GPT show a 9-fold rightward shift in antagonist potency, relative to the presence of GPT. EC_{50} values of LY341495 were statistically different in the absence versus in the presence of GPT. For experiments represented in both panels, relative increases in LY341495 efficacy were observed in the presence of GPT. Cells were incubated in DMEM buffer in the absence or presence of GPT for 4 hours prior to assay. EC_{50} values were calculated using the 4-parameter logistic equation. Statistical significance was assessed using a two-tailed Student's *t*-test. Data are presented as the mean \pm S.E.M. of three individual experiments performed in triplicate.

Figure 3. Chloride activates mGlu3, mGlu4, mGlu6, and mGlu8, but not mGlu2, receptors. **(A)** cAMP levels in CHO-Glo cells were unaffected by 10 μ M LY341495 or 1 mM glutamate, regardless of chloride concentration. **(B)** cAMP levels in mGlu2-Glo cells were reduced by glutamate, but unaffected by LY341495 or chloride. **(C-F)** cAMP levels in mGlu3-, mGlu4-, mGlu6-, and mGlu8-Glo cells were reduced by 1 mM glutamate, and by chloride in a concentration-dependent manner. Chloride EC₅₀ values were calculated to be 29.0 mM, ~275 mM, ~120 mM, and 21.1 mM at mGlu3, mGlu4, mGlu6, and mGlu8 receptors, respectively. Data were normalized independently at each chloride concentration to the maximal cAMP resulting from either LY341495, vehicle, or glutamate treatment. Gray bars represent the physiological range of chloride, from 95 to 125 mM. EC₅₀ values were calculated using the 4-parameter logistic equation. Data are presented as the mean \pm S.E.M. of three individual experiments performed in triplicate and are summarized in **Supplemental Table 2**.

Figure 4. The chloride binding site at mGlu3 receptors is disrupted at mGlu2 receptors. **(A-D)** mGlu3 and mGlu2 receptors are represented in pale-yellow and pale-blue, respectively. Glutamate (**Data Supplement 1**) is displayed as a mesh surface with gray carbons, and chloride (actually a water molecule from agonist-bound structures, **Data Supplement 2**) is green. Oxygen, nitrogen, and hydrogen atoms are red, blue, and white, respectively. **(A)** The glutamate-bound crystal structure of the mGlu3 receptor ECD (PDB ID: 2E4U) illustrates the proximity of the orthosteric glutamate and chloride sites. **(B)** An *in silico* mGlu3 receptor model (**Data Supplement 3**), built from an agonist-bound mGlu3 receptor crystal structure (PDB ID: 2E4W), is displayed, focusing on the chloride binding pocket. Predicted interactions between chloride and T98, S149, and Y150 are magenta. **(C)** An *in silico* mGlu2 receptor homology model (**Data Supplement 4**), generated from our mGlu3 receptor model, shows no predicted interactions between chloride and S91, S143, and Y144. **(D)** An overlay of these models demonstrates a backbone shift at mGlu2 receptors (pale-blue arrow), versus mGlu3 receptors (pale-yellow arrow), which disrupts the chloride site at mGlu2 receptors. **(E)** cAMP levels modulated by 100 μ M glutamate or 10 μ M LY341495 in wild-type mGlu3-Glo cells were significantly different in 125 mM versus 4.6 mM chloride, relative to vehicle treatment. However, cAMP levels modulated by glutamate or LY341495 in mGlu3 receptor T98D mutant-Glo cells were less affected by chloride. Data are presented as the mean \pm S.E.M.

of three individual experiments performed in triplicate. Statistical significance was assessed using a two-tailed Student's *t*-test. * $P < 0.05$, *** $P < 0.001$.

Figure 5. Chloride is both an agonist and a positive modulator of glutamate-mediated group II and III mGlu receptor activity. **(A-D)** Concentration-response curves of glutamate in the presence of increasing chloride concentrations (determined for each receptor based on chloride EC_{50} values from **Fig. 3**) show an increase in basal cAMP inhibition (E_0) at low glutamate concentrations, but no change in maximal cAMP inhibition (E_{max}) at high glutamate concentrations. The EC_{50} of glutamate was significantly decreased in the absence of chloride at mGlu4 and mGlu6 receptors, but was statistically unaffected by chloride at mGlu3 and mGlu8 receptors. **(E)** A table of E_0 , E_{max} , and EC_{50} values highlights statistical differences. All data were normalized as a percent of maximal cAMP levels in the absence of chloride. E_0 , E_{max} , and EC_{50} values were calculated using the 4-parameter logistic equation. Statistics were calculated using a one-way ANOVA with a Bonferroni post-hoc test, where statistical significance was defined at $P < 0.05$. Data are presented as the mean \pm S.E.M. of three individual experiments performed in triplicate. ** $P < 0.01$, *** $P < 0.001$.

Figure 6. An “Arginine Flip” dictates chloride discrimination between mGlu2 and mGlu3 receptors. **(A)** Overlay of *in silico* mGlu3 (pale-yellow) and mGlu2 (pale-blue) receptor models reveals strikingly different conformations of R277/R271. This “Arginine Flip” (curved arrow) alters the conformation of Y150/Y144, which causes a backbone to diverge between mGlu2 (pale-blue arrow) and mGlu3 (pale-yellow arrow) receptors. Glutamate (gray carbons, **Data Supplement 1**) illustrates proximity to the orthosteric glutamate site. **(B)** The mGlu3 receptor model (pale-yellow) shows a π -cation interaction between R277 and Y150, and that D279 (E273 at mGlu2 receptors) stabilizes the conformation of R277 via a salt bridge. The mGlu2 receptor homology model (pale-blue) shows that the “Arginine Flip” precludes a π -cation interaction with Y144 because R271 is stabilized by a salt bridge with D146 (S152 at mGlu3 receptors). Furthermore, this overlay of glutamate (**Data Supplement 1**), chloride (**Data Supplement 2**), mGlu3 (pale-yellow, **Data Supplement 3**), and mGlu2 (pale-blue, **Data Supplement 4**) receptor models illustrates the structural differences that chloride exploits to selectively activate mGlu3, but not mGlu2,

receptors. At mGlu3 receptors, the orientation of Y150 aligns S149 and T98 appropriately to bind chloride. At mGlu2 receptors however, the conformation of Y144 facilitates a backbone shift (pale-blue arrow), relative to mGlu3 receptors (pale-yellow arrow), which disrupts the chloride binding site. Glutamate is displayed as a mesh surface (gray carbons) to convey proximity to the orthosteric glutamate site. Oxygen, nitrogen, hydrogen, and molecular interactions are colored red, blue, white, and magenta, respectively.

Figure 7. A single amino acid mutation acts as a molecular switch for chloride sensitivity. **(A,B)** Chloride-response curves for wild-type mGlu2 and mGlu3 receptors are reproduced from **Figure 3** for comparison. Remaining panels show chloride-response curves at **(C)** the mGlu2 receptor D146S mutant, **(D)** the mGlu3 receptor S152D mutant, and **(E)** the mGlu3 receptor S152D/D279E mutant. All mutant receptors responded to 1 mM glutamate. Data were normalized independently at each chloride concentration to the maximal cAMP resulting from either LY341495, vehicle, or glutamate treatment. Gray bars represent the physiological range of chloride (95 to 125 mM). Curves were fit using the 4-parameter logistic equation. Data are the mean \pm S.E.M. of three experiments performed in triplicate.

Figure 1

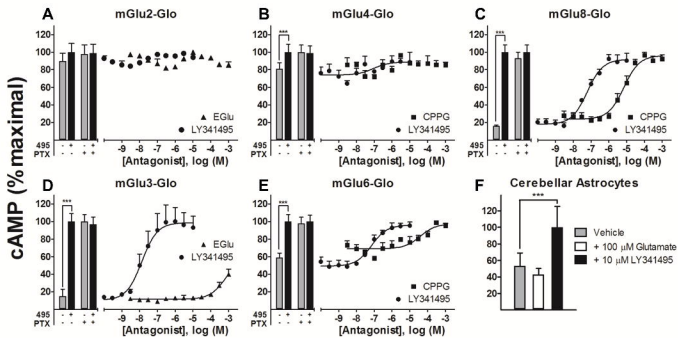


Figure 2

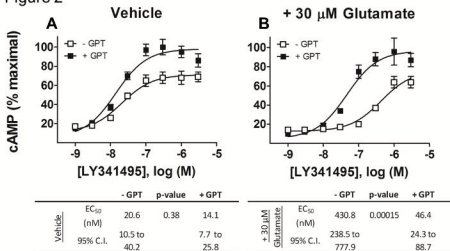


Figure 3

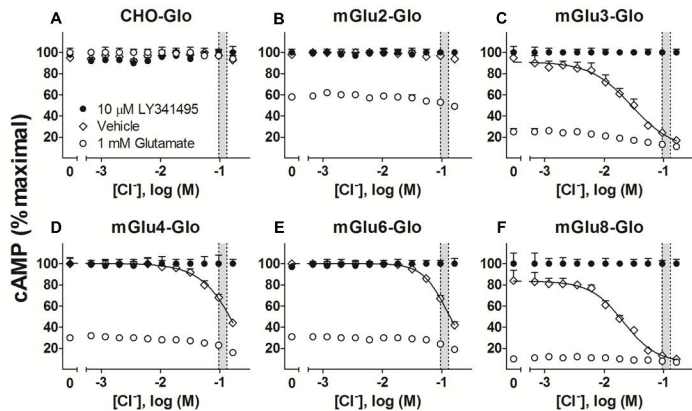


Figure 4

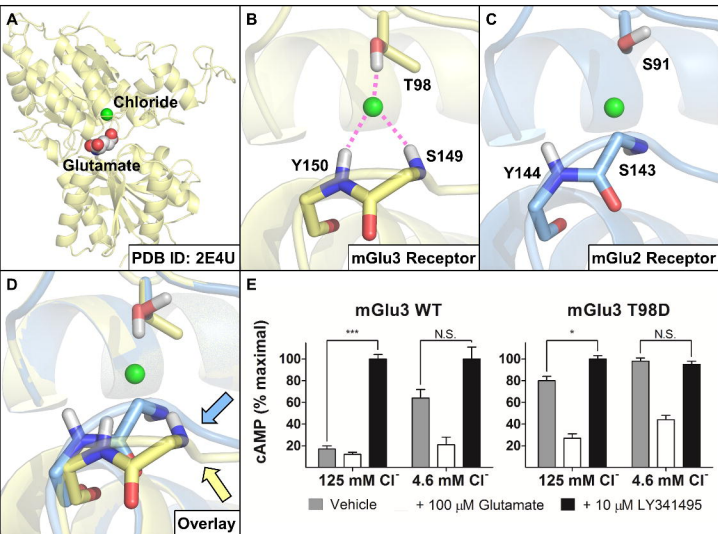


Figure 5

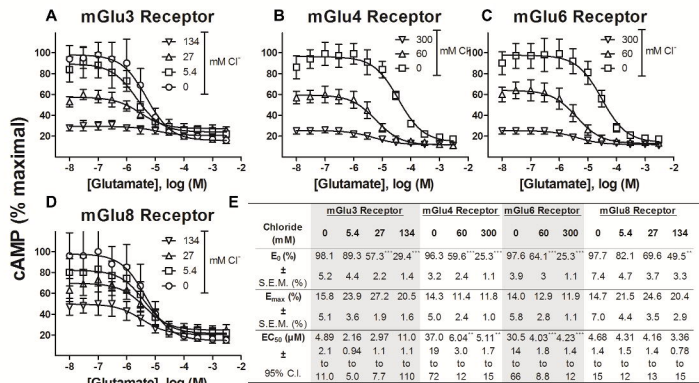


Figure 6

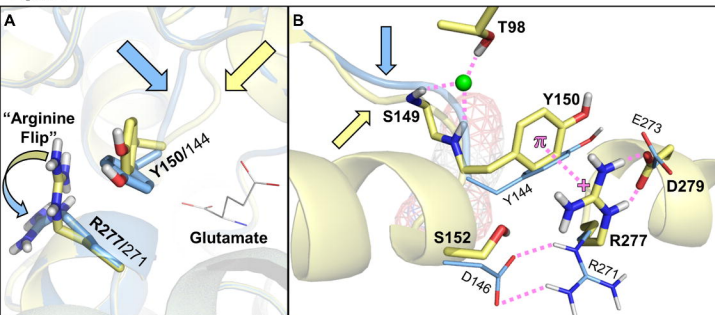


Figure 7

